Published in final edited form as:
Mol Pharm. 2014 November 3; 11(11): 4007–4014. doi:10.1021/mp500306k.

In Vivo Tumor Vasculature Targeted PET/NIRF Imaging with TRC105(Fab)-Conjugated, Dual-Labeled Mesoporous Silica Nanoparticles

Feng Chen[†], **Tapas R. Nayak**[†], **Shreya Goel**[‡], **Hector F. Valdovinos**[§], **Hao Hong**, **Charles P. Theuer**[†,∥], **Todd E. Barnhart**[§], and **Weibo Cai**[*,†,‡,§,⊥]

[†]Department of Radiology, University of Wisconsin—Madison, Madison, Wisconsin 53792, United States

[‡]Materials Science Program, University of Wisconsin—Madison, Madison, Wisconsin 53706, United States

[§]Department of Medical Physics, University of Wisconsin—Madison, Madison, Wisconsin 53705, United States

[∥]TRACON Pharmaceuticals, Inc., San Diego, California 92122, United States

[⊥]University of Wisconsin Carbone Cancer Center, Madison, Wisconsin 53792, United States

Abstract

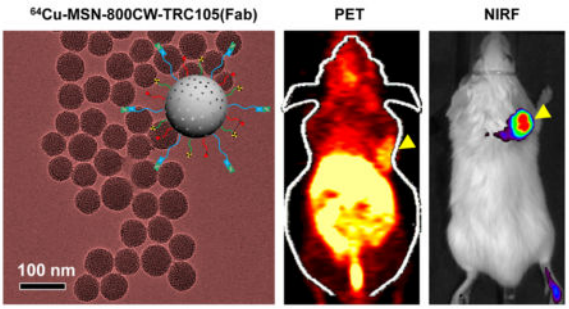

Multifunctional mesoporous silica nanoparticles (MSN) with well-integrated multimodality imaging properties have generated increasing research interest in the past decade. However,

[*]Corresponding Author: wcai@uwhealth.org. Departments of Radiology and Medical Physics, University of Wisconsin—Madison, Room 7137, 1111 Highland Avenue, Madison, Wisconsin 53705–2275, United States.

Author Contributions

Feng Chen and Tapas R. Nayak contributed equally to this work. The manuscript was written by F. Chen and W. Cai. All authors have given approval to the final version of the manuscript.

Notes

The authors declare the following competing financial interest(s): Charles P. Theuer is an employee of TRACON. The other authors declare no competing financial interest..

ASSOCIATED CONTENT

Supporting Information

Ninhydrin testing, tables of PET region-of-interest quantifications, quantitative analysis of PET imaging data from non-targeted and blocking groups. This material is available free of charge via the Internet at http://pubs.acs.org.

limited progress has been made in developing MSN-based multimodality imaging agents to image tumors. We describe the successful conjugation of, copper-64 (^{64}Cu, $t_{1/2}$ = 12.7 h), 800CW (a near-infrared fluorescence [NIRF] dye), and TRC105 (a human/murine chimeric IgG1 monoclonal antibody) to the surface of MSN via well-developed surface engineering procedures, resulting in a dual-labeled MSN for in vivo targeted positron emission tomography (PET) imaging/NIRF imaging of the tumor vasculature. Pharmacokinetics and tumor targeting efficacy/specificity in 4T1 murine breast tumor-bearing mice were thoroughly investigated through various in vitro, in vivo, and ex vivo experiments. Dual-labeled MSN is an attractive candidate for future cancer theranostics.

Keywords

vasculature targeting; positron emission tomography (PET) imaging; near-infrared fluorescence (NIRF) imaging; mesoporous silica nanoparticle (MSN)

INTRODUCTION

Vasculature targeting of tumor angiogenesis can be done based on biomarkers on the surface of tumor endothelial cells and does not require nanoparticle extravasation.[1] Vasculature targeted ligands, including vascular endothelial growth factor (VEGF) and arginine–glycine–aspartic acid (RGD) peptides, have been conjugated to the surface of different functional nanoparticles, including but not limited to, quantum dots (QDs),[2] single-walled carbon nanotubes (SWNTs),[3] and nanographene oxide (GO),[4,5] for enhanced tumor targeted imaging and drug delivery.

TRC105 (a human/murine chimeric IgG1 monoclonal antibody) is a promising vasculature targeting moiety,[6] which binds to both human and murine CD105 (endoglin), a vascular-specific marker for tumor angiogenesis.[7,8] Using TRC105 antibody and its fragments (i.e., TRC105(Fab) or F(ab′)$_2$), we reported the first positron emission tomography (PET) imaging of CD105 expression in cancer,[9,10] demonstrating the potential of CD105 for cancer-targeted imaging and therapy.

Fluorescence imaging, especially near-infrared fluorescence (NIRF) imaging, is economical and highly sensitive in certain scenarios. However, it is not quantitative in nature.[11] PET imaging, in contrast, has superb tissue penetration of signal, high sensitivity, and quantitative evaluation of the in vivo biodistribution.[12] The combination of PET with NIRF may provide more complementary information than either single modality alone and has attracted increasing interests recently.[13–20] For example, to mitigate the qualitative nature of QDs optical imaging, copper-64 (^{64}Cu, $t_{1/2}$ = 12.7 h) labeled QDs have been developed for in vivo PET/NIRF targeted dual-modality imaging using RGD peptides as the targeting ligands.[13]

Mesoporous silica nanoparticle (MSN) possesses many attractive properties and have been intensively investigated as a novel and biocompatible drug delivery system.[21–24] Although MSN itself emits no light, many strategies have been developed for engineering fluorescent MSN that can be tracked by optical imaging. For example, fluorescent dyes with varied

excitation/emission combinations have been chemically linked to the surface or loaded into the matrix of MSN for studying the dynamic distribution of MSN in vivo.[25,26] Moreover, optical nanocrystals, including QDs[27] and upconversion nanoparticles,[28] have also been encapsulated into MSN for imaging deeper tissues. Efforts have focused on the design of various fluorescent MSNs for in vivo cancer imaging, but little progress has been made with respect to in vivo tumor targeted imaging of the functionalized MSN.

Herein, using TRC105 (Fab) vascular targeting moiety as the targeting ligand, we report the first example of ^{64}Cu (a PET tracer) and 800CW (a NIRF dye) labeled MSN for PET/NIRF dual-modality imaging of the tumor vasculature. Pharmacokinetics and tumor targeting efficacy/specificity in 4T1 murine breast tumor-bearing mice were thoroughly investigated through various in vitro, in vivo, and ex vivo experiments. Our dual-labeled MSN could become a promising candidate for future image-guided drug delivery and targeted cancer therapy.

EXPERIMENTAL SECTION

Materials

TRC105 was provided by TRACON Pharmaceuticals Inc. (San Diego, CA). PD-10 columns were purchased from GE Healthcare (Piscataway, NJ). IR Dye 800CW-NHS (NHS denotes *N*-hydroxysuccinimide) ester was acquired from LI-COR Biosciences Co. (Lincoln, NE). SCM-PEG$_{5k}$-Mal was obtained from Creative PEGworks. NOTA-SCN (i.e., 2-S-(4-isothiocyanatobenzyl)-1,4,7-triazacyclononane-1,4,7-triacetic acid) was acquired from Macrocyclics, Inc. (Dallas, TX). NHS-fluorescein, Chelex 100 resin (50–100 mesh), tetraethyl orthosilicate (TEOS), ammonia ($NH_3 \cdot H_2O$), triethylamine (TEA), 3-aminopropyl)triethoxysilane (APS), dimethyl sulfoxide, cetyltrimethylammonium chloride (CTAC, 25 wt %), and Kaiser test kit were purchased from Sigma-Aldrich (St. Louis, MO). Traut's reagent (2-Iminothiolane·HCl) and Ellman's reagent (5,5′-dithiobis(2-nitrobenzoic acid) or DTNB) were purchased from Fisher Scientific. Water and all buffers were of Millipore grade and pretreated with Chelex 100 resin to ensure that the aqueous solution was free of heavy metals. All chemicals were used as received without further purification.

Generation of TRC105(Fab)

Procedures for the synthesis of TRC105(Fab) were the same as we reported previously.[29] Typically, TRC105 (2 mg/mL) was digested out in a reaction buffer (20 mM sodium phosphate monobasic, 10 mM disodium ethylenediaminetetraacetic acid [EDTA], and 80 mM cysteine hydrochloride) for 4 h at 37 °C, with immobilized papain/TRC105 at a weight ratio of 1:40. Afterward, the reaction mixture was centrifuged at 5000*g* for 1 min to remove the immobilized papain. The supernatant was purified by size exclusion column chromatography on a Sephadex G-75 column to yield TRC105(Fab), using phosphate-buffered saline (PBS) as the mobile phase.

For the thiolation of TRC105(Fab), in 700 μL (1.5 mg/mL) of TRC105(Fab) was added 50 μL (2 mg/mL) of Traut's reagent and adjusted the pH to 8.0 using 0.1 M Na_2CO_3. The mixture was kept shaking for 2 h at room temperature. As-synthesized TRC105(Fab)-SH was purified using PD-10 columns with PBS as the mobile phase. Fraction from 3.0 to 4.0

mL was collected and concentrated using a 10 k filter at 5000 rpm for 15 min. The final concentration of TRC105-(Fab)-SH was found to be about 1.7 mg/mL (~300 μL).

Synthesis of MSN

Procedures for the synthesis of ~80 nm sized MSN were the same as we reported previously.[30] In a typical synthesis, CTAC (2 g) and TEA (20 mg) were dissolved in 20 mL of high Q water and stirred at room temperature for 1 h. Afterward, 1.0 mL of TEOS was added rapidly and the resulting mixture was stirred for 1 h at 95 °C in a water bath. The mixture was then cooled down, collected by centrifugation, and washed with water and ethanol to remove residual reactants. Subsequently, the product was extracted for 24 h with a 1 wt% solution of NaCl in methanol at room temperature to remove the template CTAC. This process was carried out for at least three times to ensure complete removal of CTAC.

For amino group modification, as-synthesized MSN was first dispersed in 20 mL of absolute ethanol, followed by addition of 1 mL of APS. The system was sealed and kept at 86–90 °C in a water bath for 48 h. Afterward, the mixture was centrifuged and washed with ethanol for several times to remove the residual APS. The MSN-NH_2 could be well-dispersed in water, and the concentration of –NH_2 groups (nmol/mL) was measured using a Kaiser test kit.

Synthesis of NOTA-MSN-800CW-PEG-TRC105(Fab)

To conjugated MSN with 800CW, 2 nmol of 800CW-NHS ester was mixed with MSN-NH_2 (with ~100 nmol of –NH_2 groups) and reacted for 2 h at room temperature (pH 8.5–9.0) to form MSN-800CW-NH_2. Then, NOTA-SCN (~53 nmol) in dimethyl sulfoxide was allowed to react with MSN-800CW-NH_2 at pH 8.5 to obtain NOTA-MSN-800CW-NH_2. Afterward, 2 mg (400 nmol) of SCM-PEG_{5k}-Mal was added and reacted for another 2 h, resulting in NOTA-MSN-800CW-PEG-Mal. NOTA-MSN-800CW-PEG-TRC105(Fab) could be obtained by reacting TRC105(Fab)-SH with NOTA-MSN-800CW-PEG-Mal at room temperature for overnight. The final sample was kept at 4 °C before ^{64}Cu labeling. Note, both “NOTA” and “PEG” were omitted from the acronyms of the final nanoconjugates for clarity considerations in the following sections.

Flow Cytometry

Cells were first harvested and suspended in cold PBS with 2% bovine serum albumin at a concentration of 5×10^6 cells/mL and then incubated with fluorescein conjugated MSN-800CW-TRC105(Fab) (targeted group) or fluorescein conjugated MSN-800CW (non-targeted group) for 30 min at room temperature. The cells were washed three times with cold PBS and centrifuged for 5 min. Afterward, the cells were washed and analyzed using a BD FACSCalibur four-color analysis cytometer, which is equipped with 488 and 633 nm lasers (Becton-Dickinson, San Jose, CA) and FlowJo analysis software (Tree Star, Ashland, OR). A “blocking” experiment was also performed in cells incubated with the same amount of fluorescein conjugated MSN-800CW-TRC105(Fab), where 500 μg/mL of unconjugated TRC105 was added to evaluate the CD105 specificity of fluorescein conjugated MSN-800CW-TRC105(Fab).

Radiolabeling with ^{64}Cu

$^{64}CuCl_2$ (74–148 MBq) was diluted in 300 μL of 0.1 M sodium acetate buffer (pH 6.5) and added to MSN-800CW-TRC105(Fab) or MSN-800CW. Note, all MSN nanoconjugates were already conjugated with NOTA. The reaction was allowed to proceed at 37 °C for 30 min with constant stirring. ^{64}Cu-MSN-800CW-TRC105(Fab) and ^{64}Cu-800CW-MSN were purified using PD-10 columns with PBS as the mobile phase. The radioactivity fractions (typically between 3.5 and 4.5 mL) were collected for further in vivo imaging experiments. After 6 mL of PBS, the unreacted ^{64}Cu started to elute from the column.

4T1 Murine Breast Cancer Model

All animal studies were conducted under a protocol approved by the University of Wisconsin Institutional Animal Care and Use Committee. To generate the 4T1 tumor model, 4–5 week old female BALB/c mice were purchased from Harlan (Indianapolis, IN, USA), and tumors were established by subcutaneously injecting 2×10^6 cells, suspended in 100 μL of 1:1 mixture of RPMI 1640 and Matrigel (BD Biosciences, Franklin Lakes, NJ, USA), into the front flank of mice. The tumor sizes were monitored every other day, and the animals were subjected to in vivo experiments when the tumor diameter reached 5–8 mm.

PET/NIRF Imaging and Biodistribution Studies

PET scans at various time points postinjection (pi) using a microPET/microCT Inveon rodent model scanner (Siemens Medical Solutions USA, Inc.), image reconstruction, and region-of-interest (ROI) analysis of the PET data were performed similarly to that described previously.[31] Quantitative PET data were presented as percentage injected dose per gram of tissue (%ID/g). Tumor-bearing mice were each injected with 5–10 MBq of ^{64}Cu-MSN-800CW-TRC105(Fab) or ^{64}Cu-MSN-800CW via tail vein before serial PET scans. Another group of three 4T1 tumor-bearing mice were each injected with 1 mg of unlabeled TRC105 at 1 h before ^{64}Cu-MSN-800CW-TRC105(Fab) administration to evaluate the CD105 specificity of ^{64}Cu-MSN-800CW-TRC105(Fab) in vivo (i.e., blocking experiment).

After the last PET scans at 48 h pi, biodistribution studies were carried out to confirm that the %ID/g values based on PET imaging truly represented the radioactivity distribution in tumor-bearing mice. Mice were euthanized, and blood, 4T1 tumor, and major organs/tissues were collected and wet-weighed. The radioactivity in the tissue was measured using a gamma-counter and presented as %ID/g (mean ± SD).

For in vivo NIRF imaging, each 4T1 tumor-bearing mouse was injected with MSN-800CW-TRC105(Fab) (targeted group) with the amount of 800CW estimated to be ~400 pmol. The mouse was then imaged using an IVIS spectrum in vivo imaging system (Ex = 745 nm, Em = 800 nm) at 4 h pi. For non-targeted and blocking groups, mice were injected with MSN-800CW and MSN-800CW-TRC105(Fab) (together with 1 mg blocking dose of free TRC105), respectively, with equal amount of 800CW dyes.

RESULTS AND DISCUSSION

Synthesis and Characterizations of Thiolated TRC105-(Fab)

Thiolated TRC105(Fab), i.e., TRC105(Fab)-SH, was generated following our previous reported procedures with an addition thiolation step (Figure 1a).[29] After papain digestion of full TRC105 antibody, a Sephadex G 75 column was used to separate TRC105(Fab) from other components in the reaction mixture. Sodium dodecyl sulfate polyacrylamide gel electrophoresis (SDS-PAGE) was then used to confirm the successful generation of TRC105(Fab), where the disappearance of the TRC105 band (~148 kDa, lane 2 in Figure 1b) and the appearance of pure TRC105(Fab) band (~47.5 kDa, lane 3 in Figure 1b) were shown. Traut's reagent was later used for the thiolation of TRC105(Fab), forming TRC105(Fab)-SH. The presence of –SH groups was further confirmed by using Ellman's reagent. Taken together, these results indicate the complete digestion of TRC105 after papain treatment to yield high purity TRC105(Fab) and the successful thiolation of TRC105(Fab) to form TRC105(Fab)-SH for further bio-conjugations.

Synthesis and Characterizations of ^{64}Cu-MSN-800CW-TRC105(Fab)

Multiple steps of surface engineering were required for the synthesis ^{64}Cu-MSN-800CW-TRC105(Fab), as shown in Scheme 1. As-synthesized uniform MSN (**1**) was first functionalized with amino groups (–NH_2) with (3-aminopropyl)triethoxysilane (APS), to form MSN-NH_2 (**2**), leaving amino groups on the surface for further conjugation. Successful –NH_2 modification was confirmed by ninhydrin testing (Supportiong Information Figure S1). The desired amount of NIRF dyes (800CW-NHS ester) and NOTA-SCN (a ^{64}Cu chelator) and were then reacted with MSN-NH_2 at pH 8.5–9 to produce NOTA-MSN-800CW-NH_2 (**3**). Afterward, the heterobifunctional succinimidyl carboxy methyl ester-poly ethylene glycol(5 kDa)-maleimide (SCM-PEG_{5k}-Mal) was used to generate NOTA-MSN-800CW-PEG-Mal (**4**), which was then reacted with TRC105(Fab)-SH to yield NOTA-MSN-800CW-PEG-TRC105(Fab) (**5**). Lastly, the NOTA-MSN-800CW-PEG-TRC105(Fab) was labeled with ^{64}Cu to form the ^{64}Cu-NOTA-MSN-800CW-PEG-TRC105(Fab) nanoconjugate (**6**), abbreviated as ^{64}Cu-MSN-800CW-TRC105(Fab). Because all the MSN nanoconjugates will contain the same NOTA and PEG chains (5 kDa), both "NOTA" and "PEG" were omitted from the acronyms of the final nanoconjugates for clarity.

Figure 2a shows the representative transmission electron microscopy (TEM) image of ~80 nm sized uniform MSN, which was synthesized following as described.[30] No obvious changes in the morphology of MSN were observed after multistep surface modifications, as evidenced by TEM image of MSN-800CW-TRC105(Fab) (Figure 2b). Successful conjugation of 800CW to MSN was confirmed by the NIRF imaging of MSN-800CW-TRC105(Fab) (inset in Figure 2b) using the IVIS spectrum in vivo imaging system (Ex = 745 nm, Em = 800 nm). Dynamic light scattering (DLS) and ζ potential measurements indicated the final *Z-average* size and surface charge of MSN-800CW-TRC105(Fab) to be 175.3 ± 9.7 nm and −3.25 ± 0.8 mV (pH 7.4, PBS), respectively.

In Vitro CD105 Targeting of MSN-800CW-TRC105-(Fab)

Previously, we have demonstrated that fluorescein conjugated TRC105(Fab) binds with high avidity and specificity to human umbilical vein endothelial cells (HU-VECs),[29] indicating that papain digestion does not affect antigen recognition. To assess CD105 targeting efficiency of MSN nanoconjugates, a flow cytometry study using HUVECs was also performed after NHS-fluorescein was conjugated to the surface of nanoparticles. Flow cytometry results (Figure 3) indicated that incubation with fluorescein conjugated MSN-800CW-TRC105(Fab) significantly enhanced the mean fluorescence intensity of HUVECs, compared to fluorescein conjugated MSN-800CW. The specificity of in vitro CD105 targeting with MSN-800CW-TRC105(Fab) was confirmed in the blocking study, where only background level uptake of MSN-800CW-TRC105(Fab) was observed after blocking HUVECs with a large dose of free TRC105 (500 μg/mL).

In Vivo PET/NIRF Dual Modal CD105-Targeted Imaging of ^{64}Cu-MSN-800CW-TRC105(Fab)

For in vivo tumor targeted PET imaging, both MSN-800CW-TRC105-(Fab) and MSN-800CW were labeled with ^{64}Cu for in vivo imaging and biodistribution studies. As-synthesized ^{64}Cu-MSN-800CW-TRC105(Fab) (targeted group) and ^{64}Cu-MSN-800CW (non-targeted group) were purified using PD-10 columns with PBS as the mobile phase. The radioactivity fractions (typically elute between 3.0 and 4.0 mL) were collected for in vivo experiments. Unreacted ^{64}Cu eluted from the column by the 6 mL fractions.

In vivo tumor targeted imaging was carried out in 4T1 murine breast tumor-bearing mice, which express a high level of CD105 on the tumor neovasculature.[7,8] Each mouse was intravenously (iv) injected with 5–10 MBq of ^{64}Cu-MSN-800CW-TRC105(Fab) or MSN-800CW-TRC105(Fab) (had ~400 pmol of dyes) for PET/NIRF imaging to show in vivo biodistribution pattern as well as tumor accumulation (Figures 4, 5 and 6). Non-targeted and blocking groups were also included to assess the targeting specificity of dual-labeled MSN nanoconjugates. Quantitative data obtained from ROI analysis of these PET images are also shown in Supporting Information Table S1–S3.

The accumulation of ^{64}Cu-MSN-800CW-TRC105(Fab) in the 4T1 tumor was clearly demonstrated in PET imaging and was found to be 5.4 ± 0.2%ID/g at 4 h pi, as shown in Figures 4a and 6a and Supporting Information Table S1 (n = 3). In contrast, the 4T1 tumor uptake of ^{64}Cu-MSN-800CW was found to be ~2%ID/g at all of the time points examined (n = 3; Figure 4b, Supporting Information Figure S2a and Table S2), indicating that TRC105(Fab) conjugation was required for enhanced tumor accumulation of ^{64}Cu-MSN-800CW-TRC105-(Fab) in vivo. To further confirm the CD105 targeting specificity of ^{64}Cu-MSN-800CW-TRC105(Fab), blocking studies were performed. The administration of a blocking dose (1 mg/mouse) of free TRC105 at 1 h before ^{64}Cu-MSN-800CW-TRC105(Fab) injection significantly reduced tumor uptake to 2.3 ± 0.2%ID/g at 4 h pi (n = 3, Figure 4c, Supporting Information Figure S2b and Table S3), demonstrating the CD105 specific targeting of ^{64}Cu-MSN-800CW-TRC105(Fab) in vivo. Figure 6c further summarizes the comparison of 4T1 tumor uptake of three groups at different time points. ^{64}Cu-MSN-800CW-TRC105(Fab) showed the highest tumor uptake throughout the study period.

In vivo NIRF imaging was used to further confirm the enhanced accumulation of MSN-800CW-TRC105(Fab). Different MSN nanoconjugates which contained equal amounts of dyes (~400 pmol) were injected intravenously into 4T1 tumor-bearing mice. In vivo NIRF images that were generated at 4 h pi (when the nanoparticles showed the highest tumor accumulation based on the PET imaging, shown in Figure 4a) were acquired and are shown in Figure 5. A significantly stronger signal from the targeted group was observed compared to the non-targeted and blocking groups, indicating the successful detection by NIRF imaging of MSN-800CW-TRC105(Fab) nanoconjugates. Notably, the liver and spleen were the major organs for the accumulation of MSN-800CW-TRC105(Fab). However, due to the difference in scattering behaviors and depth, only 800CW emission signalsfrom xenograft 4T1 tumor on the surface of mouse skin were detected by the IVIS spectrum in vivo imaging system. Taken together, these data demonstrated the CD105 specificity of dual-modality PET/NIRF targeted imaging using ^{64}Cu-MSN-800CW-TRC105-(Fab) in vivo.

The conjugate ^{64}Cu-MSN-800CW-TRC105(Fab) also improved tumor-to-muscle (T/M) biodistribution ratios. As shown in Figure 6b, T/M value of the targeted group was estimated to be 5.2 ± 0.2 at 0.5 h pi and increased up to 7.3 ± 1.1 at 4 h pi, which was significantly higher than that of non-targeted and blocking groups (Supporting Information Figure S2c,d and Table S4–S6). Similar to other TRC105-conjugated nanoparticles,[4,5,30] besides tumor accumulation, most of the ^{64}Cu-MSN-800CW-TRC105(Fab) nanoconjugates were cleared by the reticuloendothelial system (RES) with liver uptake found to be 23.2 ± 3.5%ID/g at 0.5 h pi, decreasing gradually to 9.2 ± 0.6%ID/g by 48 h pi (n = 3; Figures 4a and 6a, and Supporting Information Table S1), which was validated by the ex vivo biodistribution study (Figure 6d). Similar trends were also observed in the non-targeted and blocking groups (Supporting Information Figure S2a,b and Table S2–S3).

CONCLUSION

In conclusion, we report the in vivo tumor vasculature targeted PET/NIRF dual-modality imaging using well-functionalized ^{64}Cu-MSN-800CW-TRC105(Fab) nanoconjugates. Pharmacokinetics and tumor targeting efficacy/specificity in 4T1 murine breast tumor-bearing mice were thoroughly investigated through various in vitro, in vivo, and ex vivo experiments. Vascular targeting led to ~2-fold enhancement of tumor accumulation over passive targeting alone. Other targeting ligands could also be conjugated to MSN for further improvement of tumor accumulation in vivo. Given the presence of tunable pore size and larger surface area that could accommodate therapeutic agents, as-designed ^{64}Cu-MSN-800CW-TRC105(Fab) could be employed as both imaging and therapeutic agents.

Supplementary Material

Refer to Web version on PubMed Central for supplementary material.

Acknowledgments

This work is supported, in part, by the University of Wisconsin—Madison, the National Institutes of Health (NIBIB/NCI 1R01CA169365, P30CA014520), the Department of Defense (W81XWH-11-1-0644), and the American Cancer Society (125246-RSG-13-099-01-CCE).

References

1. Chen F, Cai W. Tumor Vasculature Targeting: A Generally Applicable Approach for Functionalized Nanomaterials. Small. 2014; 10:1887–1893. [PubMed: 24591109]
2. Cai W, Shin DW, Chen K, Gheysens O, Cao Q, Wang SX, Gambhir SS, Chen X. Peptide-Labeled Near-Infrared Quantum Dots for Imaging Tumor Vasculature in Living Subjects. Nano Lett. 2006; 6:669–676. [PubMed: 16608262]
3. Liu Z, Cai W, He L, Nakayama N, Chen K, Sun X, Chen X, Dai H. In Vivo Biodistribution and Highly Efficient Tumour Targeting of Carbon Nanotubes in Mice. Nature Nanotechnol. 2007; 2:47–52. [PubMed: 18654207]
4. Hong H, Yang K, Zhang Y, Engle JW, Feng L, Yang Y, Nayak TR, Goel S, Bean J, Theuer CP, Barnhart TE, Liu Z, Cai W. In Vivo Targeting and Imaging of Tumor Vasculature with Radiolabeled, Antibody-Conjugated Nanographene. ACS Nano. 2012; 6:2361–2370. [PubMed: 22339280]
5. Shi S, Yang K, Hong H, Valdovinos HF, Nayak TR, Zhang Y, Theuer CP, Barnhart TE, Liu Z, Cai W. Tumor Vasculature Targeting and Imaging in Living Mice with Reduced Graphene Oxide. Biomaterials. 2013; 34:3002–3009. [PubMed: 23374706]
6. Rosen LS, Hurwitz HI, Wong MK, Goldman J, Mendelson DS, Figg WD, Spencer S, Adams BJ, Alvarez D, Seon BK, Theuer CP, Leigh BR, Gordon MS. A Phase I First-in-Human Study of TRC105 (Anti-Endoglin Antibody) in Patients with Advanced Cancer. Clin Cancer Res. 2012; 18:4820–9. [PubMed: 22767667]
7. Seon BK, Haba A, Matsuno F, Takahashi N, Tsujie M, She X, Harada N, Uneda S, Tsujie T, Toi H, Tsai H, Haruta Y. Endoglin-Targeted Cancer Therapy. Curr Drug Delivery. 2011; 8:135–143.
8. Fonsatti E, Nicolay HJ, Altomonte M, Covre A, Maio M. Targeting Cancer Vasculature Via Endoglin/CD105: A Novel Antibody-Based Diagnostic and Therapeutic Strategy in Solid Tumours. Cardiovasc Res. 2010; 86:12–19. [PubMed: 19812043]
9. Hong H, Yang Y, Zhang Y, Engle JW, Barnhart TE, Nickles RJ, Leigh BR, Cai W. Positron Emission Tomography Imaging of CD105 Expression During Tumor Angiogenesis. Eur J Nucl Med Mol Imaging. 2011; 38:1335–1343. [PubMed: 21373764]
10. Hong H, Zhang Y, Orbay H, Valdovinos HF, Nayak TR, Bean J, Theuer CP, Barnhart TE, Cai W. Positron Emission Tomography Imaging of Tumor Angiogenesis with a (61/64)Cu-Labeled F(ab′) (2) Antibody Fragment. Mol Pharm. 2013; 10:709–716. [PubMed: 23316869]
11. James ML, Gambhir SS. A Molecular Imaging Primer: Modalities, Imaging Agents, and Applications. Physiol Rev. 2012; 92:897–965. [PubMed: 22535898]
12. Gambhir SS. Molecular Imaging of Cancer with Positron Emission Tomography. Nature Rev Cancer. 2002; 2:683–693. [PubMed: 12209157]
13. Cai W, Chen K, Li ZB, Gambhir SS, Chen X. Dual-Function Probe for PET and Near-Infrared Fluorescence Imaging of Tumor Vasculature. J Nucl Med. 2007; 48:1862–1870. [PubMed: 17942800]
14. Chen K, Li ZB, Wang H, Cai W, Chen X. Dual-Modality Optical and Positron Emission Tomography Imaging of Vascular Endothelial Growth Factor Receptor on Tumor Vasculature Using Quantum Dots. Eur J Nucl Med Mol Imaging. 2008; 35:2235–2244. [PubMed: 18566815]
15. Lee J, Lee TS, Ryu J, Hong S, Kang M, Im K, Kang JH, Lim SM, Park S, Song R. RGD Peptide-Conjugated Multimodal $NaDdF_4$:Yb^{3+}/Er^{3+} Nanophosphors for Upconversion Luminescence, MR, and PET Imaging of Tumor Angiogenesis. J Nucl Med. 2013; 54:96–103. [PubMed: 23232276]

16. Sun Y, Yu M, Liang S, Zhang Y, Li C, Mou T, Yang W, Zhang X, Li B, Huang C, Li F. Fluorine-18 Labeled Rare-Earth Nanoparticles for Positron Emission Tomography (PET) Imaging of Sentinel Lymph Node. Biomaterials. 2011; 32:2999–3007. [PubMed: 21295345]
17. Xie J, Chen K, Huang J, Lee S, Wang J, Gao J, Li X, Chen X. PET/NIRF/MRI Triple Functional Iron Oxide Nanoparticles. Biomaterials. 2010; 31:3016–3022. [PubMed: 20092887]
18. Zhou J, Yu M, Sun Y, Zhang X, Zhu X, Wu Z, Wu D, Li F. Fluorine-18-Labeled $Gd^{3+}/Yb^{3+}/Er^{3+}$ Co-Doped $NaYF_4$ Nanophosphors for Multimodality PET/MR/UCL Imaging. Biomaterials. 2011; 32:1148–1156. [PubMed: 20965563]
19. Huang X, Zhang F, Lee S, Swierczewska M, Kiesewetter DO, Lang L, Zhang G, Zhu L, Gao H, Choi HS, Niu G, Chen X. Long-Term Multimodal Imaging of Tumor Draining Sentinel Lymph Nodes Using Mesoporous Silica-Based Nanoprobes. Biomaterials. 2012; 33:4370–4378. [PubMed: 22425023]
20. Zhang Y, Hong H, Engle JW, Yang Y, Barnhart TE, Cai W. Positron Emission Tomography and Near-Infrared Fluorescence Imaging of Vascular Endothelial Growth Factor with Dual-Labeled Bevacizumab. Am J Nucl Med Mol Imaging. 2012; 2:1–13. [PubMed: 22229128]
21. Vallet-Regi M, Rámila A, del Real RP, Pérez-Pariente J. A New Property of Mcm-41: Drug Delivery System. Chem Mater. 2000; 13:308–311.
22. Lu J, Liong M, Li Z, Zink JI, Tamanoi F. Biocompatibility, Biodistribution, and Drug-Delivery Efficiency of Mesoporous Silica Nanoparticles for Cancer Therapy in Animals. Small. 2010; 6:1794–1805. [PubMed: 20623530]
23. Meng H, Xue M, Xia T, Ji Z, Tarn DY, Zink JI, Nel AE. Use of Size and a Copolymer Design Feature to Improve the Biodistribution and the Enhanced Permeability and Retention Effect of Doxorubicin-Loaded Mesoporous Silica Nanoparticles in a Murine Xenograft Tumor Model. ACS Nano. 2011; 5:4131–4144. [PubMed: 21524062]
24. Pan L, He Q, Liu J, Chen Y, Ma M, Zhang L, Shi J. Nuclear-Targeted Drug Delivery of TAT Peptide-Conjugated Monodisperse Mesoporous Silica Nanoparticles. J Am Chem Soc. 2012; 134:5722–5725. [PubMed: 22420312]
25. Wang K, He X, Yang X, Shi H. Functionalized Silica Nanoparticles: A Platform for Fluorescence Imaging at the Cell and Small Animal Levels. Acc Chem Res. 2013; 46:1367–1376. [PubMed: 23489227]
26. Lee CH, Cheng SH, Wang YJ, Chen YC, Chen NT, Souris J, Chen CT, Mou CY, Yang CS, Lo LW. Near-Infrared Mesoporous Silica Nanoparticles for Optical Imaging: Characterization and in Vivo Biodistribution. Adv Funct Mater. 2009; 19:215–222.
27. Pan J, Wan D, Gong J. Pegylated Liposome Coated QDs/Mesoporous Silica Core–Shell Nanoparticles for Molecular Imaging. Chem Commun. 2011; 47:3442–3444.
28. Liu J, Bu W, Zhang S, Chen F, Xing H, Pan L, Zhou L, Peng W, Shi J. Controlled Synthesis of Uniform and Monodisperse Upconversion Core/Mesoporous Silica Shell Nanocomposites for Bimodal Imaging. Chemistry. 2012; 18:2335–2341. [PubMed: 22252972]
29. Zhang Y, Hong H, Orbay H, Valdovinos HF, Nayak TR, Theuer CP, Barnhart TE, Cai W. Pet Imaging of CD105/Endoglin Expression with a (6)(1)/(6)(4)Cu-Labeled Fab Antibody Fragment. Eur J Nucl Med Mol Imaging. 2013; 40:759–767. [PubMed: 23344138]
30. Chen F, Hong H, Zhang Y, Valdovinos HF, Shi S, Kwon GS, Theuer CP, Barnhart TE, Cai W. In Vivo Tumor Targeting and Image-Guided Drug Delivery with Antibody-Conjugated, Radiolabeled Mesoporous Silica Nanoparticles. ACS Nano. 2013; 7:9027–9039. [PubMed: 24083623]
31. Orbay H, Zhang Y, Valdovinos HF, Song G, Hernandez R, Theuer CP, Hacker TA, Nickles RJ, Cai W. Positron Emission Tomography Imaging of CD105 Expression in a Rat Myocardial Infarction Model with (64)Cu-Nota-TRC105. Am J Nucl Med Mol Imaging. 2013; 4:1–9. [PubMed: 24380040]

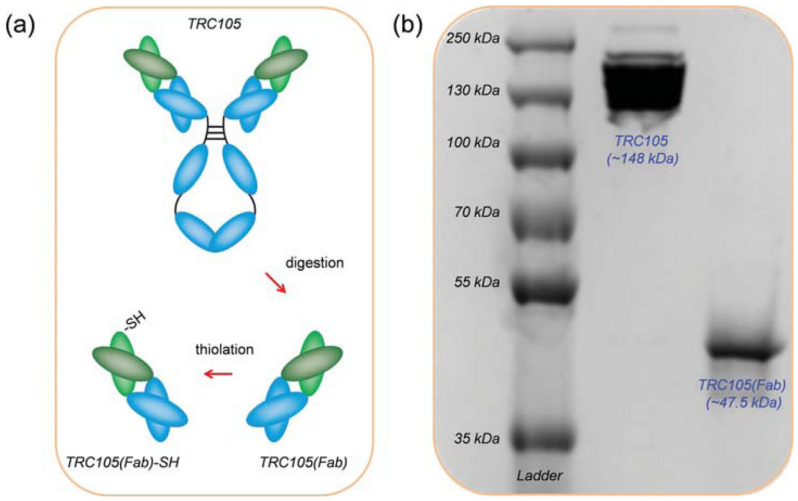

Figure 1.

Synthesis and characterization of TRC105(Fab). (a) Schematic illustration showing the generation of TRC105(Fab) and its thiolation. (b) SDS-PAGE of molecular weight markers (lane 1), intact TRC105 antibody (lane 2), and TRC105(Fab) after purification on the Sephadex G-75 column (lane 3).

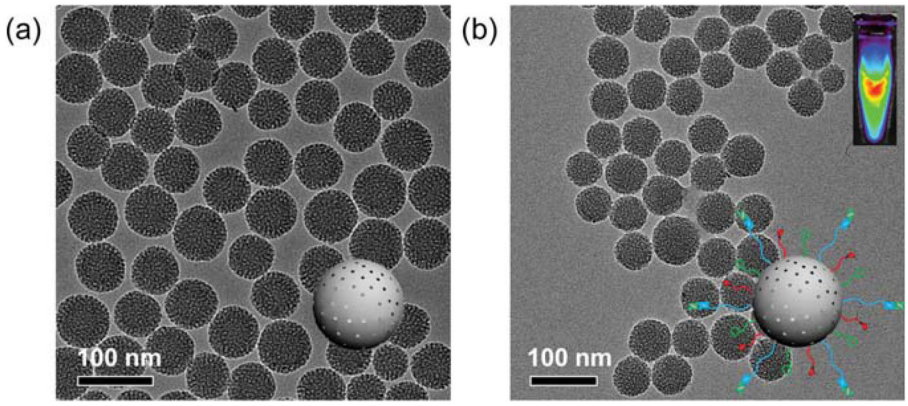

Figure 2.

Synthesis and characterization of MSN and MSN-800CW-TRC105(Fab). TEM images of (a) pure MSN, (b) MSN-800CW-TRC105(Fab). Insets in (a) and (b) show the schemes of MSN and MSN-800CW-TRC105(Fab). An optical image of MSN-800CW-TRC105(Fab) acquired from IVIS spectrum in vivo imaging system (Ex = 745 nm, Em = 800 nm) is also shown in the upper right portion of (**b**).

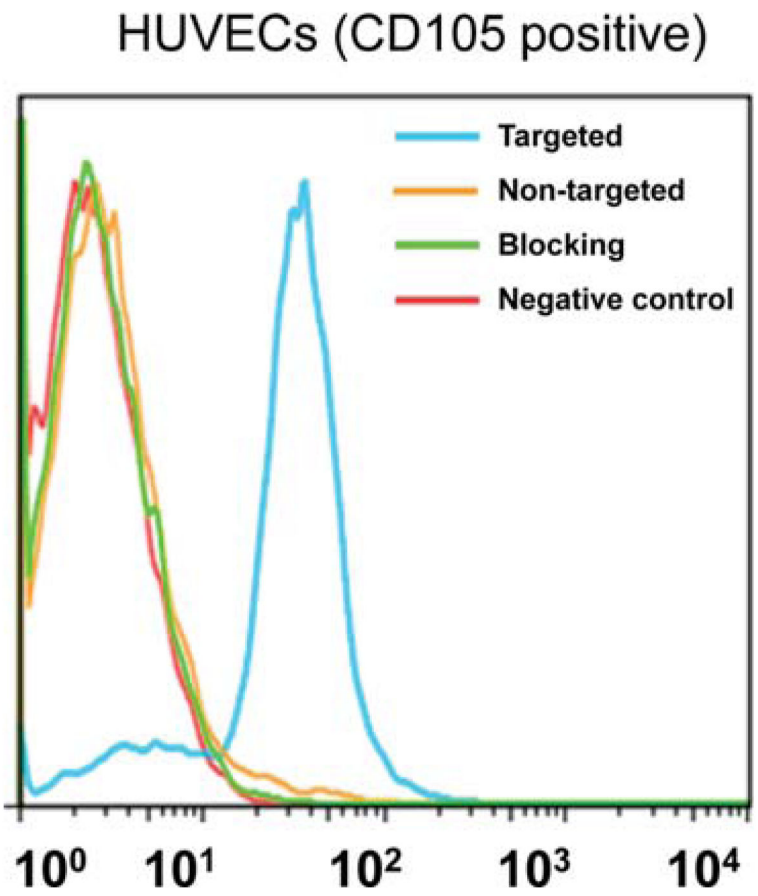

Figure 3.

Flow cytometry analysis of MSN nanoconjugates in HUVECs (CD105 positive) after 30 min incubation and subsequent washing. Targeted group: fluorescein conjugated MSN-800CW-TRC105(Fab). Non-targeted group: fluorescein conjugated MSN-800CW. Blocking group: fluorescein conjugated MSN-800CW-TRC105(Fab) with a blocking dose of TRC105 (500 μg/mL).

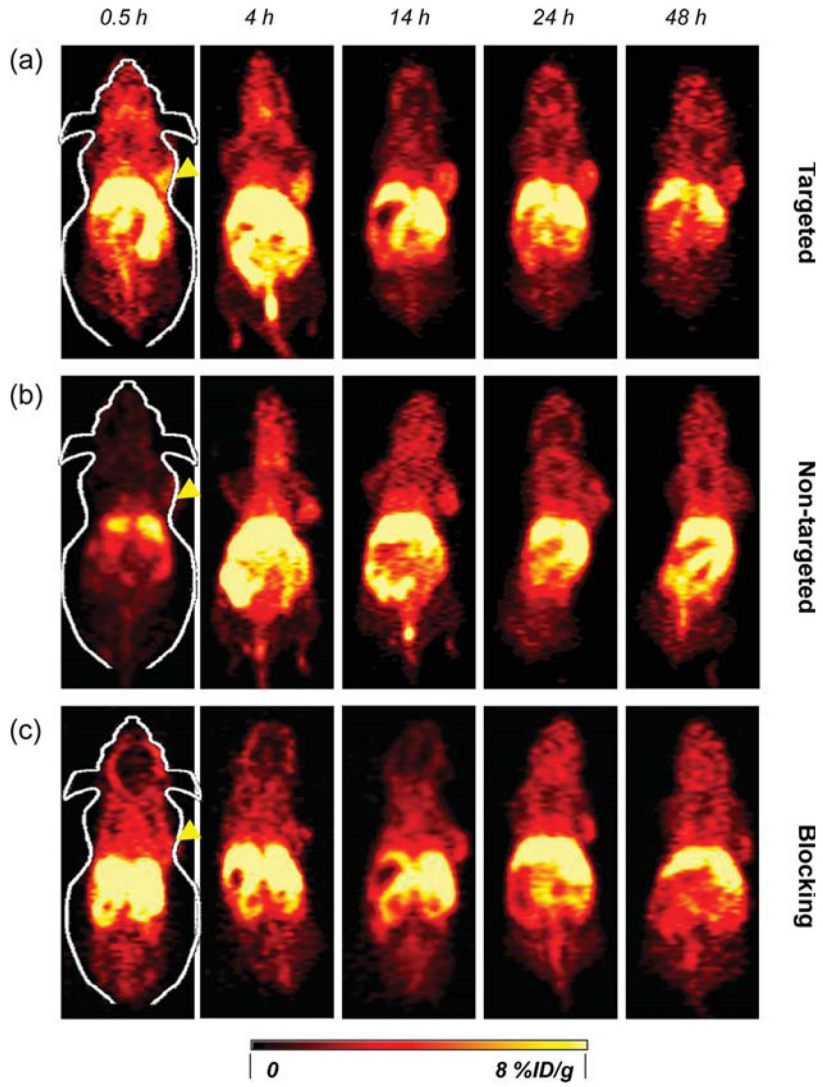

Figure 4.

Serial coronal PET images of 4T1 tumor-bearing mice at different time points postinjection of (a) ^{64}Cu-MSN-800CW-TRC105(Fab), (b) ^{64}Cu-MSN-800CW, and (c) ^{64}Cu-MSN-800CW-TRC105(Fab) with a blocking dose of TRC105 (1 mg/mouse). Tumors are indicated by yellow arrowheads.

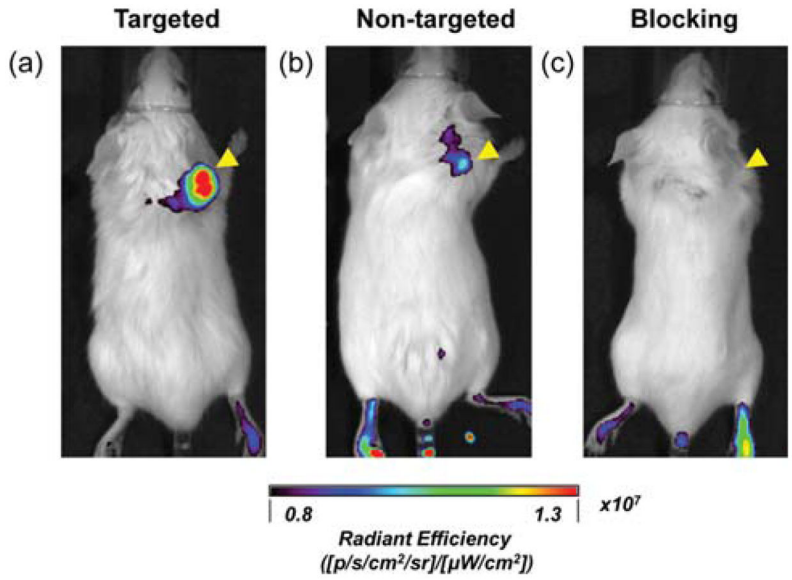

Figure 5.

In vivo NIRF imaging of 4T1 tumor-bearing mice at 4 h postinjection. (a) Targeted group, ^{64}Cu-MSN-800CW-TRC105(Fab); (b) non-targeted group, ^{64}Cu-MSN-800CW; (c) blocking group, ^{64}Cu-MSN-800CW-TRC105(Fab) with a blocking dose of TRC105 (1 mg/mouse). Tumors are indicated by yellow arrowheads. Each mouse was iv injected with MSN nanoconjugates with equal amounts of 800CW dyes (~400 pmol). All images were acquired by using IVIS spectrum in vivo imaging system (Ex = 745 nm, Em = 800 nm).

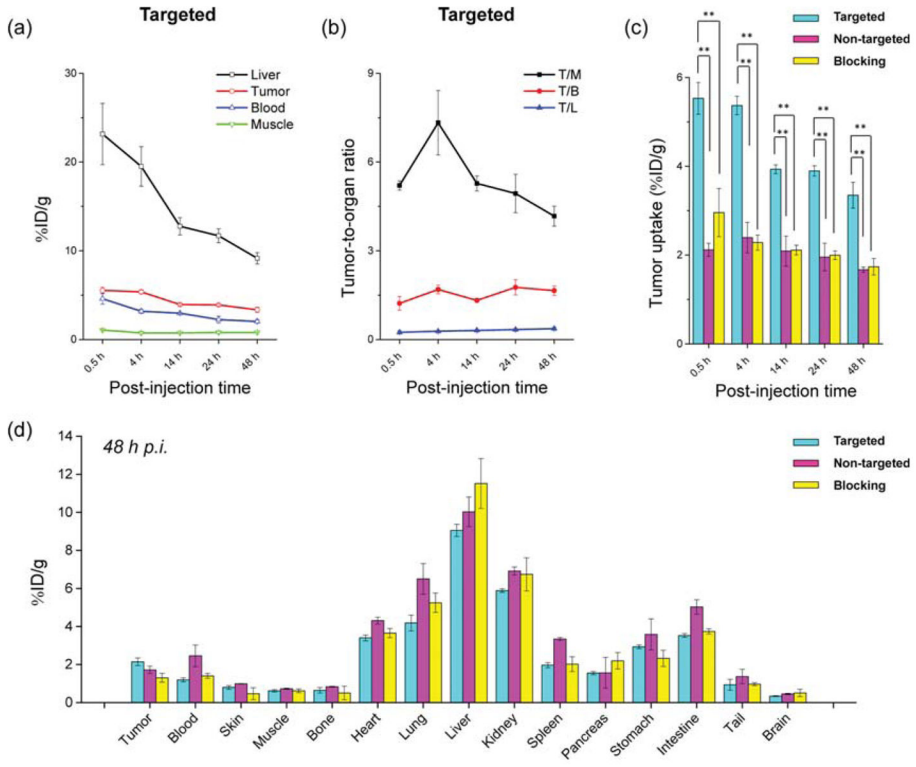

Figure 6.

Quantitative analysis of the PET data. (a) Time–activity curve of the liver, 4T1 tumor, blood, and muscle upon iv injection of ^{64}Cu-MSN-800CW-TRC105(Fab) (targeted group, n = 3). (b) Time–activity curve of tumor-to-muscle (T/M), tumor-to-blood (T/B), and tumor-to-liver (T/L) ratios from the same targeted group (n = 3). (c) Comparison of 4T1 tumor uptake among the three groups. The differences between 4T1 tumor uptake of ^{64}Cu-MSN-800CW-TRC105(Fab) and the two control groups were statistically significant (** $P <$ 0.01) in all cases. (d) Biodistribution of three groups in 4T1 tumor-bearing mice at the end of the PET scans at 48 h pi (n = 3).

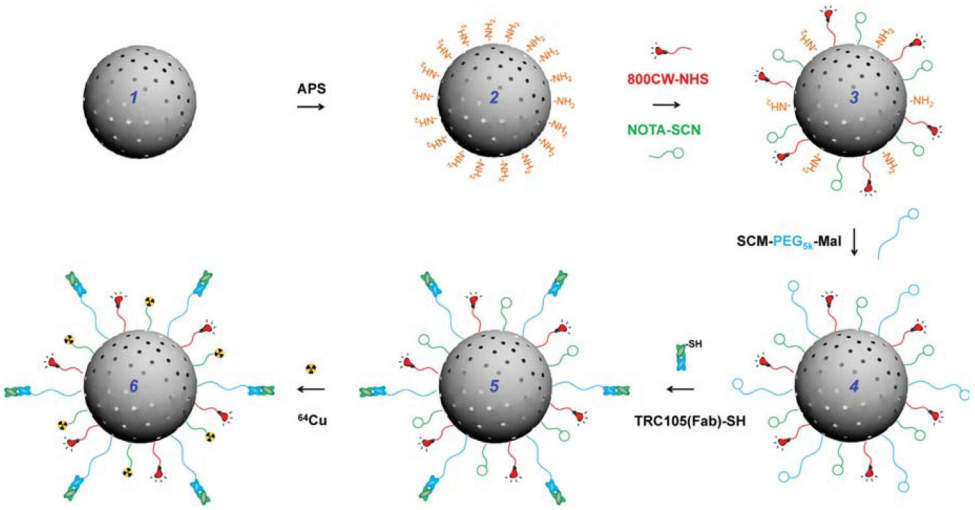

Scheme 1. Schematic Illustration of the Synthesis of ^{64}Cu-MSN-800CW-TRC105(Fab)[a]

[a]Uniform MSN nanoparticle (**1**) was first modified with –NH_2 groups with APS to form MSN-NH_2 (**2**). As-synthesized MSN-NH_2 was then subjected to 800CW and NOTA conjugation to yield NOTA-MSN-800CW-NH_2 (**3**). Afterwards, PEGylation step was introduced to render the stability of NOTA-MSN-800CW-PEG-Mal (**4**) in PBS, at the same time adding maleimide groups. NOTA-MSN-800CW-PEG-TRC105(Fab) (**5**) could be obtained by reacting TRC105(Fab)-SH with **4** at room temperature. ^{64}Cu-labeling was performed in the last step to generate ^{64}Cu-NOTA-MSN-800CW-PEG-TRC105(Fab) (**6**), short for ^{64}Cu-MSN-800CW-TRC105(Fab).